Molecular Neurobiology
https://doi.org/10.1007/s12035-024-04365-4

RESEARCH

Biflavonoid Methylchamaejasmin and *Khaya grandifoliola* Extract Inhibit NLRP3 Inflammasome in THP-1 Cell Model of Neuroinflammation

Brice Ayissi Owona[1,2] · Arnaud Mary[6] · Angelique N. Messi[3] · Kishore Aravind Ravichandran[2] · Josephine Ngo Mbing[3] · Emmanuel Pegnyemb[3] · Paul F. Moundipa[1] · Michael T. Heneka[2,4,5,6,7]

Received: 23 February 2024 / Accepted: 11 July 2024

Abstract

Neuroinflammation is a common hallmark of Alzheimer's disease (AD), with NLRP3 inflammasome proven to be activated in microglia of AD patients' brains. In this study, a newly isolated biflavonoid (7,7′-di-O-methylchamaejasmin/M8) and a crude extract of the plant *Khaya grandifoliola* (KG) were investigated for their inhibitory effect on inflammasome activation. In preliminary experiments, M8 and KG showed no cytotoxicity on human macrophage-like differentiated THP-1 cells and exhibited anti-inflammatory inhibition of nitric oxide produced following lipopolysaccharide stimulation. Furthermore, M8 and KG blocked IL-1β and IL-18 production by reducing NLRP3 inflammasome components including NFκB, NLRP3, Caspase-1, pro-IL-1β, and pro-IL-18 at the mRNA and protein levels. Regarding the formation of ASC (apoptosis-associated speck-like protein containing a CARD) specks during inflammasome activation, the size and fluorescent intensity of the existing specks were unchanged across all treatment conditions. However, M8 and KG treatments were shown to prevent further speck formation. In addition, experiments on amyloid β phagocytosis showed that M8 and KG pretreatments can restore the phagocytic activity of THP-1 cells, which was impaired following inflammasome activation. Altogether, our findings describe for the first time a promising role of biflavonoids and KG extract in preventing inflammasome activation and protecting against neuroinflammation, a key factor in AD development.

Keywords NLRP3 inflammasome · THP-1 cells · Biflavonoid · 7,7′-di-O-Methylchamaejasmin · *Khaya grandifoliola*

Abbreviations

Aβ	Amyloid beta
AD	Alzheimer's disease
ASC	Apoptosis-associated speck-like protein containing a CARD
CNS	Central nervous system
ELISA	Enzyme-linked immunosorbent assay
fAβ	Fibrillary amyloid beta
FDA	Food and Drug Administration
GFP	Green fluorescent protein
HRESIMS	High-resolution electrospray ionization mass spectroscopy

Brice Ayissi Owona and Arnaud Mary contributed equally to this work.

✉ Brice Ayissi Owona
vincent-brice.owona@facsciences-uy1.cm

✉ Michael T. Heneka
michael.heneka@uni.lu

[1] Laboratory of Pharmacology and Toxicology, Department of Biochemistry, Faculty of Science, University of Yaoundé I, AEFAS, P.O. Box 812, Yaoundé, Cameroon

[2] German Center for Neurodegenerative Diseases, Venusberg, Campus 1/Gebäude 99, 53127 Bonn, Germany

[3] Laboratory of Organic Chemistry, Faculty of Science, University of Yaoundé I, P.O. BOX 812, Yaoundé, Cameroon

[4] Institute of Physiology II, University Hospital Bonn, Nußallee 11, 53115 Bonn, Germany

[5] Institute of Innate Immunity, University Hospital, Venusberg, Campus 1/Gebäude 12, 53127 Bonn, Germany

[6] Luxembourg Centre for Systems Biomedicine, University of Luxembourg, 6 Avenue du Swing, 4367 Belvaux, Luxembourg

[7] Infectious Diseases and Immunology, University of Massachusetts Chan Medical School, 55 Lake Avenue North Worcester, Worcester, MA 01655, USA

Published online: 16 July 2024

IL-1β/18	Interleukin 1 beta/18
KG	*Khaya grandifoliola*
LPS	Lipopolysaccharide
M8	7,7′-Di-O-Methylchamaejasmin
NFκB	Nuclear factor kappa B
NFTs	Neurofibrillary tangles
NLRP3	NOD-like receptor family, pyrin domain containing 3
NO	Nitric oxide
Nrf2	Nuclear factor erythroid 2–related factor 2
NRM	Nuclear magnetic resonance
PMA	Phorbol-12-myristate-13-acetate
RT	Room temperature
RTqPCR	Reverse transcription quantitative polymerase chain reaction
TAMRA	5-Carboxytetramethylrhodamine
THP-1 cells	Human leukemia monocytic cell line
TLC	Thin-layer chromatography

Introduction

Neuroinflammation is a common hallmark of neurodegenerative disorders including Alzheimer's disease (AD) [1]. AD is clinically characterized by the deposition of intracellular tau in neurofibrillary tangles (NFTs) as well as the accumulation of amyloid β (Aβ) plaques in the brain [2]. Resident innate immune cells of the central nervous system (CNS), known as microglia, are reported to play a pivotal role in the initiation and potentiation of neuroinflammatory responses [3] and the development and progression of neurodegenerative diseases [4]. In AD patients, for instance, microglia surround Aβ plaques where they initiate the activation of inflammasome, followed by the secretion of pro-inflammatory cytokines [5]. Indeed, the NOD-LRR- and pyrin domain-containing protein 3 (NLRP3) inflammasome is the most described complex among the inflammasome family and a critical component of the innate immune system. NLRP3 inflammasome's activation causes Caspase-1 autocleavage activation and thereby the secretion of pro-inflammatory cytokines IL-18 and IL-1β [6].

Another hallmark of AD is the inhibition of the phagocytic activity of microglia. Indeed, microglial phagocytosis is known as a way of lowering Aβ load in AD [7]. Microglia interact with fibrillary Aβ (fAβ) through cell surface receptors, thereby promoting fAβ phagocytosis. In AD, fAβ initiates the destruction of phagosomes in microglia, thereby lowering their phagocytic activity and clearance capacity [8]. Therefore, research focusing on finding lead compounds that enhance microglial clearance activity despite inflammasome activation may be promising in AD drug development.

Currently, accumulated evidence has demonstrated that aberrant activation of NLRP3 inflammasome is associated with AD progression [9]. Discovering new NLRP3 inhibitors could be promising towards finding new treatments for neurodegenerative diseases involving NLRP3 inflammasome activation. Several inhibitors have been described in the literature including tranilast, OLT1177, and oridonin [10–12]. MCC950, a specific inhibitor of NLRP3 inflammasome, was reported to improve diabetes-mediated cognitive impairment and was studied in a phase II clinical trial for the treatment of rheumatoid arthritis, but the drug was discontinued due to reported liver toxicity [13]. Unfortunately, some of these drugs must be used at high doses and are not tolerated by many patients. Moreover, in addition to limited efficacy in reducing cognitive decline, currently available Food and Drug Administration (FDA)'s approved drugs including aducanumab (anti-Aβ), donepezil, rivastigmine, and galantamine have several severe side effects that further limit their clinical use.

Medicinal plants appear as a good alternative for the discovery of lead compounds against AD. Indeed, several FDA-approved drugs have been derived directly or indirectly from medicinal plants. This is the case of quinine, an alkaloid taken from *Cinchona calisaya* tree from South America, and artemisinin isolated from *Artemisia annua* for malaria treatment. Many studies have reported neuroprotective effects of flavonoids. Biflavonoids are natural compounds belonging to the family of flavonoids and are made up of two monoflavonoid residues connected by a direct connection or a linker. They are reported to have a wide range of pharmacological effects including anti-tumor [14], antioxidant [15, 16], anti-viral [17, 18], and anti-inflammatory [19] activities. In the case of AD, several flavonoids have shown great potential in disease treatment. Interestingly, due to the aromatic interaction of biflavonoids, their therapeutic effect has been reported to be stronger than that of flavonoids [20], suggesting that they can be good candidates for disease treatment. Some biflavonoids have been reported for their potential beneficial effects in AD treatment; this is the case of amentoflavone reported to inhibit the formation and accumulation of Aβ [21]. In the same line, polyphenolic biflavonoids were reported to inhibit Aβ fibrillation and to disaggregate preformed Aβ fibrils which are linked to the pathogenesis of AD [22]. Until now, the majority of studies on biflavonoids in AD have focused on their capacity to inhibit Aβ self-assembly into oligomers and fibrils [23]. Another study from the same author showed that biflavonoids can alter Aβ aggregation and even more effectively reduce the toxicity of Aβ oligomers compared to the monoflavonoid moieties [20]. However, no study has reported the effect of biflavonoids on neuroinflammation, precisely their ability to inhibit inflammasome components and limit the secretion of pro-inflammatory mediators.

7,7′-di-O-Methylchamaejasmin (M8) is a newly isolated biflavonoid which has not been extensively studied for its

pharmacological effects. The single available biological study reports its cytotoxic effects on multi-factorial drug-resistant cancer cells [24]. Its antiplasmodial and antibacterial activities were also reported in a recent study [25].

Khaya grandifoliola (KG) is a plant of the Meliaceae family growing in West Cameroon. It has been widely used by traditional healers in the country for malaria treatment. Work from our research group reported its effects against hepatitis C virus infection in vitro [26, 27] and its anti-inflammatory properties via nuclear factor erythroid-2 related factor 2 (Nrf2) transcription factor inhibition [28]. Moreover, we showed that KG is a potential source of therapeutic compounds for AD treatment [29]. Chemical compounds present in KG have been identified and include mainly limonoids (17-epi-methyl-6-hydroxylangolensate, 7-deacetoxy-7-oxogedunin, and 7-deacetoxy-7R-hydroxygedunin) [26]. Moreover, unpublished data from our research group show that further fractionation of KG leads to loss of activity in anti-inflammatory bio-guided experiments.

In our current investigation, we aimed to describe the anti-inflammatory effect of M8 and KG, two drugs used by traditional healers in Cameroon for the treatment of inflammatory and brain-related disorders, as well as studying their capacity to inhibit inflammasome components using THP-1 cells, a suitable microglia-like model for studying neuroinflammation.

Methods

Plant Material

The root barks of *Ochna schweinfurthiana* F. Hoffm (Ochnaceae) known in Cameroon as 'Sa'aboule' were collected from the Dang district in the Adamaoua region in December 2018. A voucher specimen (No. 40171HNC) was deposited at the national herbarium in Yaoundé (Cameroon).

Extraction and Isolation

Dried and powdered root bark of *Ochna schweinfurthiana* (200 g) was extracted with MeOH (3 × 3 L) at room temperature (RT) to yield a crude extract (47 g) after evaporation under vacuum. The extract (MeOH, 80 g) was subjected to column chromatography over silica gel eluting with gradients of CH_2Cl_2/MeOH to generate 10 fractions of 100 mL each. These fractions were combined based on their thin-layer chromatography (TLC) profiles into four major fractions: A (0.11 g, 1–10); B (0.30 g, 11–30); C (0.23 g, 31–60); and D (0.89 g, 61–90). Fractions A (CH_2Cl_2; 100%); B (CH_2Cl_2/MeOH; 50:1); and C (CH_2Cl_2/MeOH; 40:1) contained mostly lipids. Fraction D (CH_2Cl_2/MeOH 30:1) was purified by silica gel column chromatography with a gradient of CH_2Cl_2/MeOH (20:1) followed by a Sephadex LH20 column in acetone to generate 7,7′-di-O-methylchamaejasmin (M8) (30 mg).

General Experimental Procedures

Melting points were determined on Electro thermal IA9000 series digital melting point apparatus and were uncorrected. The UV spectra were recorded on UV-570/VIS/NIP (Thermo Scientific Cat#ND-ONE-W) and Shimadzu UV-24012A double-beam spectrophotometers. IR measurements were obtained on a PerkinElmer model 1600 FTIR spectrometer (PerkinElmer Cat#PE1600). The 1D (^{1}H, ^{13}C, DEPT) and 2D (COSY, NOESY, HSQC, and HMBC) NMR spectra were recorded in MeOH-d_4 using a Bruker 400 (400 MHz for ^{1}H-NMR, 100 MHz for ^{13}C-NMR) spectrometer. HRESIMS spectra were obtained from MSQ Thermo Finnigan instrument. Chemical shifts were stated in parts per million (ppm) from the internal standard, tetramethylsilane (TMS). Flash column chromatography was performed using silica gel 60 (Merck, 0.040 − 0.063 mm). TLC was conducted on pre-coated Merck Kieselgel 60 F_{254} plates (20 × 20 cm, 0.25 mm). Spots were checked on TLC plates under UV light (254 nm), and developed with vanillin reagent, followed by heating.

Khaya grandifoliola Hydro-ethanol Extract Preparation

The stem bark of KG was harvested in July 2018 in the Foumban district, West Cameroon, and identified at the national herbarium in Yaoundé where a specimen is kept under the reference number 23434YA. After that, plant barks were washed using tap water, air-dried, and ground. Five hundred grams of the powder was weighed and extracted at room temperature (25 °C) using 2 L of the ethanol–water (65:35 V/V) solvent system for 48 h with constant shaking. The mixture was filtered using a Whatman No. 1 filter paper, and the residue was re-extracted twice using the same solvent mixture. The filtrate was pooled and concentrated under reduced pressure with a rotary evaporator to remove ethanol traces. The crude extract obtained was dried using a dry oven at 40 °C to obtain the hydro-ethanolic extract of KG.

MTT Assay to Determine Cytotoxicity

To study the potential cytotoxic effect of M8 and KG on THP-1 cells, we used the 3-(4,5-dimethylthiazol-2-yl)-2,5-diphenyltetrazolium bromide (MTT)-based colorimetric assay for the non-radioactive quantification of cell proliferation and viability (Roche Cat#11465007001). Cells (5×10^5 cells/well) were grown in a 96-well tissue culture plate,

treated with 150 nM PMA (phorbol-12-myristate-13-acetate) (Sigma-Aldrich Cat#P1585), and left to adhere for 24 h. Subsequently, 200 µL of fresh RPMI culture medium was mixed with 30 µL of the yellow MTT (5 mg/mL) solution and incubated at 37 °C and 5% CO_2 for 4 h. After this incubation period, the culture medium was aspirated, and the purple formazan crystals formed were solubilized using 50 µL of DMSO in each well. The solubilized formazan product was spectrophotometrically quantified by reading its absorbance at 560 nm using an ELISA plate reader (TECAN Infinite M200 Plate Reader). The percentage of cell viability was calculated as compared to the control considered 100% viability.

Measurement of Nitric Oxide (NO) Production

The production of NO was determined by measuring the levels of nitrite accumulation, an indicator of NO in cell culture supernatant after 24 h of treatment [30]. THP-1 cells (5×10^5 cells/well) were treated with PMA and allowed to adhere to 96-well culture plates for 24 h. On the following day, cells were treated with LPS (0.1 µg/mL) + nigericin (10 mM), M8 (10, 20, and 40 µM), and KG (12.5, 25, 50, 100 µg/mL) and incubated in RPMI medium for 24 h. Control wells were treated with RPMI medium only. Sulfanilamide and NED (naphtyl ethylene diamine) solutions were allowed to equilibrate at RT for 30 min. Afterwards, 50 µL of each experimental sample was added to the wells of new 96-well plates in triplicate. Using a multichannel pipettor, 50 µL of the sulfanilamide solution was distributed to all experimental samples and wells containing the dilution series of the nitrite standard which served as reference curve. The plates were incubated for 10 min at RT, protected from light. Fifty microliters of the NED solution was then added to all wells and the plates were incubated for another 10 min at RT, protected from light. The absorbance of the purple-colored solution formed was measured in a plate reader at 550 nm (TECAN Infinite M200 Plate Reader).

Enzyme-Linked Immunosorbent Assay (ELISA) for Supernatant Cytokine Quantification

THP-1 cells (5×10^5 cells/well) were treated with 150 nM PMA and allowed to adhere to a 96-well culture plate for 24 h. On the following day, cells were treated with LPS (0.1 µg/mL) + nigericin (10 mM) + M8 (10, 20, and 40 µM) or KG (12.5, 25, 50, 100 µg/mL) and incubated in RPMI medium for 24 h. After this incubation period, supernatants were collected for the following ELISA assays: human IL-18 (R&D systems Cat#DY318-05) and IL-1β/IL-1F2 (R&D systems Cat#DY201) DuoSet ELISA. The capture antibody solution was diluted to the working concentration (1:200) in PBS without carrier protein. Immediately, a 96-well microplate was coated with 50 µL per well of the diluted captured antibody. The plate was sealed and incubated at 4 °C overnight. The next day, each well was aspirated and washed three times with 200 µL wash buffer (0.05% PBST). The plate was blocked by adding 150 µL of reagent diluent (1% BSA) to each well and incubated for 1 h. After another wash series as previously described, 50 µL of sample or standards was added. The plate was incubated for another 2 h at RT. Afterwards, aspiration/wash steps were repeated as described above, and 50 µL of the detection antibody, diluted in reagent diluent, was added to each well and incubated for 2 h at RT. After an additional series of aspiration/wash steps, 50 µL of the working dilution of streptavidin-HRP was added to each well and incubated for 20 min. Fifty microliters of substrate solution was added to each well and incubated for 20 min at RT. Finally, 25 µL of stop solution (2 N sulfuric acid) was added to each well and the optical density (OD) was read at 540 nm using a microplate reader (TECAN Infinite M200 Plate Reader).

TAMRA Amyloid β Phagocytosis Assay

To study the effect of M8 and KG on phagocytosis activity after inflammasome activation, the following protocol was used. THP-1 cells at 5×10^5 cells/well were seeded in a 96-well plate and treated with 150 nM PMA for 24 h. The medium was discarded, and the cells were treated with 90 µL ± LPS (3.5 h) + nigericin (30 min) + M8 or KG (30 min). Afterwards, 10 × TAMRA-Aβ (2.5 µM) was prepared and 10 µL was added to the wells. Nine wells were prepared and treated with RPMI only and used as control. The plate was incubated for 4 h and spun and the supernatant was discarded. One hundred microliters of trypan blue solution diluted in PBS (1:10) was added to the wells. The plate was spun, and the supernatant was discarded. Immediately, the measurement of the plate OD was taken and noted as reading 1 (540-nm excitation–585-nm emission). In the meantime, a Hoechst staining solution (25 µL in 10 mL of 0.1% Triton + PBS) was prepared and 100 µL of Hoechst was added and incubated in the dark for 15 min. The staining was discarded, and the plate was read once more (reading 2: 360-nm excitation–418-nm emission). Result = Reading 1/Reading 2. All the values calculated were relative to control untreated cells.

RNA Extraction and Reverse Transcription and Quantitative PCR (RTqPCR) for Gene Expression

THP-1 cells were cultured in Roswell Park Memorial Institute (RPMI) 1640 medium containing 10% FBS (fetal bovine serum) and 1% P/S (penicillin/streptomycin) at 37 °C and 5% CO_2. Cells were then plated at 5×10^5 cells/well density in a six-well plate in RPMI 1640 containing 1% P/S and 50 nM

PMA, respectively. Subsequently, cells were treated either with the medium only for controls or with LPS (0.1 µg/mL) for 2 h, + nigericin (10 mM) for 30 min, and afterwards M8 or KG for another 2 h. Total RNA was extracted and purified from treated THP-1 cells using the RNEasy Kit (Qiagen Cat#74,004). Afterwards, RNA samples were transcribed into cDNA as follows. Samples were prepared to get 200 ng RNA/sample (measured on the nanodrop (Thermo Scientific Cat#ND-ONE-W)). A 2XRT Master Mix was prepared using kit components and 20 µL of 2XRT Master Mix was mixed into each PCR tube. Thereafter, 20 µL of RNA sample (concentration 400 ng/20 µL) was pipetted into each well and the tubes were loaded into a thermal cycler. Afterwards, the generated cDNA products were stored at − 20 °C.

For gene expression quantification, qPCR reactions were performed using the TaqMan Gene Expression Assay kit (Applied Biosystems Cat#4,331,182) and were performed inside a StepOne™ Real-Time PCR System (Applied Biosystems Cat#4,376,357). Genes investigated included NFκB (Thermo Fisher Hs00765730_m1), NLRP3 (Thermo Fisher Hs00918082_m1), Caspase-1 (Thermo Fisher Hs00354836_m1), IL-1β (Thermo Fisher Hs01555410_m1), and IL-18 (Thermo Fisher Hs01038788_m1). In each experiment, 100 ng of cDNA was used per 20 µL of amplification reaction. Each primer solution contained forward and reverse primers and a FAM-labelled MGB TaqMan probe for each gene. 18S ribosomal RNA was used as endogenous control (VIC labelled).

Western Blot

THP-1 cells were plated at 5×10^5 cells/well in a six-well plate in RPMI 1640 containing 1% P/S and 50 nM PMA, respectively. To activate inflammasome, cells were treated either with the medium only for controls or with LPS (0.1 µg/mL) for 2 h, + nigericin (10 mM) for 30 min, and thereafter M8 or KG for another 2 h. For lysate preparation, cells were washed with PBS and 150 µL 1 × RIPA (ristocetin-induced platelet agglutination) buffer (25 mM Tris-HCl, 150 mM NaCl, 0.5% sodium desoxycholate, 1% NP-40, and 0.1% SDS) supplemented with 1 × protease/phosphate inhibitor cocktail for 20 min. Thereafter, cells were scraped off the well plate and centrifuged at 21,000 *g*, 15 min, 4 °C. Lysates obtained were denatured at 95 °C for 5 min in a thermocycler. Protein concentration was determined using the bicinchoninic (BCA) method according to the manufacturer's protocol (Thermo Scientific Cat#23,225). Thereafter, protein samples were separated on NuPAGE™ 4 to 12%, Bis–Tris, 1.0–1.5 mm, Mini Protein Gels (Invitrogen Cat#NP0324BOX), transferred unto a 0.2-µm nitrocellulose membrane (BIO-RAD Cat#1,704,158) using the Trans-Blot Turbo Transfer System (BIO-RAD Cat#1,704,150). Membranes were then blocked with TBS containing 0.05% Tween-20 in PBS (PBST) and 5% non-fat milk (in PBST) for 1 h. Afterwards, the membrane was incubated with primary antibodies (anti-NLRP3, NFκB, Caspase-1, or pro-Caspase-1) overnight at 4 °C.

Primary Antibodies for Western Blotting

Mouse anti-Caspase-1 (Bally-1); 1:2000 (Adipogen; AG-20B-0048, RRID: AB_2490257). Mouse anti-IL-1β/IL-F2; 1:1000 (R&D systems; MAB201, RRID: AB_358006. Rabbit anti-NLRP3; 1:1000 (Abcam; ab263899, RRID: AB_2889890). Rabbit anti-ASC; 1:1000 (Adipogen; AG-25B-0006 RRID: AB_2490440). Rabbit anti-Gasdermin-D; 1:1000 (Cell signaling technologies; 97,558, RRID: AB_2864253). Mouse anti-β-Actin (BA3R); 1:5000 (Invitrogen; MA5-15,739, RRID: AB_10979409).

On the next day, the membrane was washed three times for 5 min with PBST and incubated with respective secondary antibodies for 1 h at RT. The membrane was then visualized for protein quantification using a chemiluminescence machine (LI-COR Odyssey CLx Imager).

ASC Speck Detection

Briefly, 0.25×10^6 THP-1-ASC-GFP cells [31] per well of a 24-well plate were cultured in RPMI 1640, supplemented with 10% FBS (Thermo Fisher Scientific Cat#10,500,064) and 1% penicillin–streptomycin (Thermo Fisher Scientific Cat#15,140,122). The cells were differentiated with 100 nM PMA (Merck Cat#P8139) for 2 days followed by 3 days of rest in fresh media without PMA. In the required wells, the cells were pretreated 3 h with 40 µM M8 or 40 µg/mL KG, followed by a 3-h treatment of 1 µg/mL LPS (Merck Cat#L4391) followed by 90 min of 15 µM of nigericin (Life Technologies Cat#N1495). At the end of the treatment, the specks were imaged under a Zeiss Axio Observer 7 microscope (light source: LED-Module 475 nm, intensity 20%, illumination between 450 and 488 nm, objective: EC Plan-Neofluar 5 × /0.16 M27, imaging device Axiocam 705, exposure time 150 ms) in an incubation box keeping the cells alive at 37 °C, 5% CO_2, and 80% humidity. After the acquisition, the culture media were collected and 2×10^5 1 µm size, 1.35×10^5 2 µm size, and 0.9×10^5 6 µm size calibration non-fluorescent beads (Life Technologies Cat#F13838) were added. The media were then analyzed in a BD LSR-Fortessa Flow Cytometer (FSC voltage 350 V and 200 V for the threshold, SSC voltage 280 V, and Alexa Fluor voltage 530 V). Only the events of 1-µm size or less were gated on the FSC versus SSC scatter plot in order to include the debris-sized ASC specks and to exclude cells. Debris-sized $A488^+$ events were counted as ASC specks. The acquisition was performed until at least 2000 debris-sized $A488^+$ events were captured. Data were analyzed with FlowJo software

(RRID: SCR_008520). Three independent experiments were performed, with each time two to three wells per condition.

ASC Speck Quantification

ASC-GFP specks were quantified from the microscope images using ImageJ software (RRID: SCR_003070). A threshold was applied to remove the background signal and only the particles ranging from 2 to 50 µm were considered ASC-GFP specks. The number and their sizes were quantified. From the Flow Cytometer acquisition, the mean and median intensity of the debris-sized $A488^+$ were quantified.

Statistical Analysis

For statistical analysis, values obtained in each experiment have been expressed as mean ± standard deviation (SD). The statistical significance was determined using one-way ANOVA followed by Tukey's post hoc test, and $p < 0.05$ was considered statistically significant. Analysis was performed using GraphPad PRISM 8.0.2 software (San Diego, CA, USA; RRID: SCR_002798).

Results

Identification of the Isolated Compound

The crude (CH_2Cl_2/MeOH 1:1) extract of the root bark of *Ochna schweinfurthiana* was chromatographed using silica gel and Sephadex LH-20 columns to yield the pure 7,7′-di-O-methylchamaejasmin biflavonoid (M8). The isolated compound was identified using HRESIMS, NMR spectroscopy, and optical rotation measurements (Fig. 1).

Effect of M8 and KG on Cell Viability and Inhibition of LPS-Induced NO Production

We first studied the effect of 24-h LPS treatments on THP-1 cell viability using the MTT assay and found that no cytotoxicity was observed at 50 µg/mL and 100 µg/mL in comparison to the control with no LPS (Fig. 2A). Analysis of the possible cytotoxic effect of M8 and KG on human macrophage-like differentiated THP-1 cells performed by MTT assay indicated that M8, even at 40 µM, did not affect the cell viability as shown in Fig. 2B. The same was observed with KG at concentrations up to 100 µg/mL (Fig. 2C). M8 and KG effect on LPS-induced NO production in THP-1

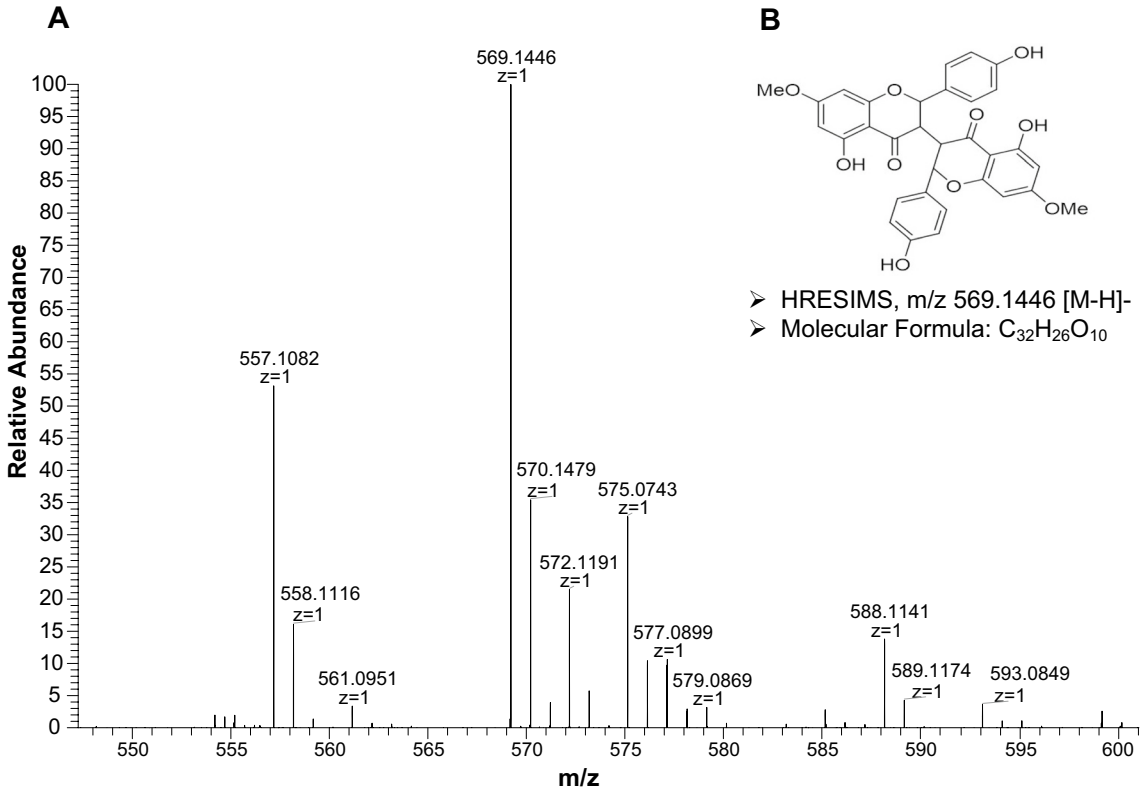

Fig. 1 HRESISM spectrum of compound M8. **A** Mass spectrometry and **B** chemical structure of compound M8 ($C_{32}H_{26}0_{10}$)

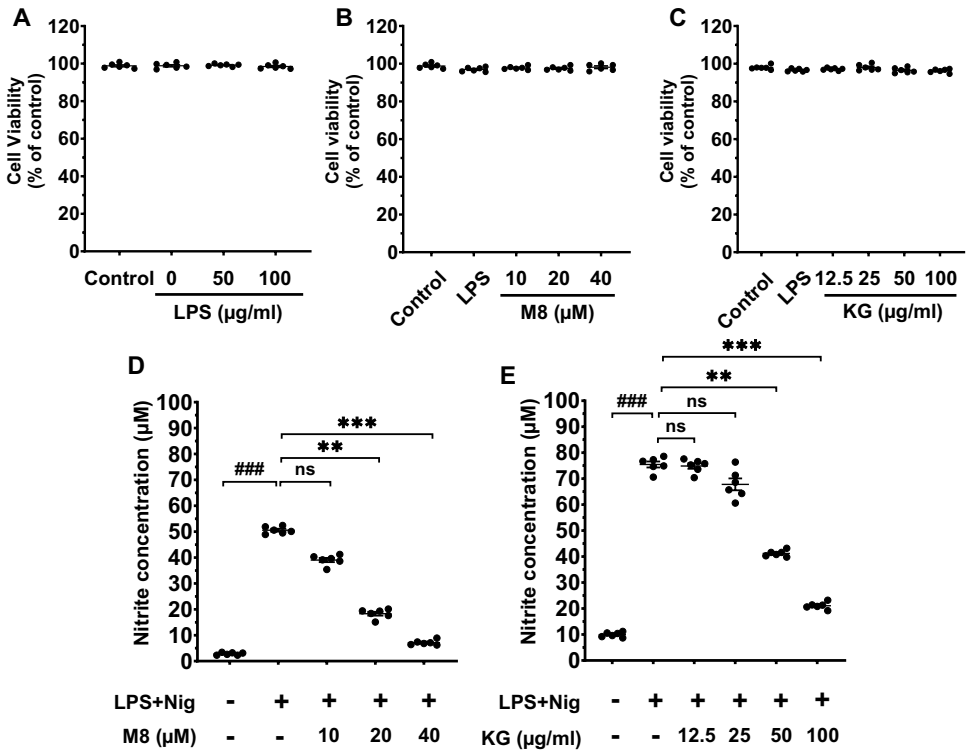

Fig. 2 MTT and nitric oxide assay. **A** Effect of LPS on THP-1 cell viability. Each dot is the median of one-well cell culture supernatant from 2 independent experiments with 3 wells per treatment condition ($n=6$). ns, non-significant ($p=0.76$, $F=4.021$, df = 3) by one-way ANOVA followed by Tukey's multiple comparison test. **B** + **C** Effect of M8 and KG on the viability of LPS-induced cells. THP-1 cells were grown in complete RPMI medium containing penicillin, streptomycin, and 10% FCS at 37 °C and 5% CO_2. 5×10^5 cells were seeded into 24-well cell culture plates and cultured for 24 h. Thereafter, 5×10^5 cells/mL were incubated with the indicated concentrations of M8 or KG, in the presence or absence of LPS 100 ng/mL for 24 h. The cell viability was then determined by MTT assay as described in the "Methods" section. **D** + **E** Effect of M8 and KG on nitric oxide production. THP-1 cells were grown in complete RPMI medium containing penicillin, streptomycin, and 10% FCS at 37 °C and 5% CO_2. 5×10^5 cells were seeded into 24-well cell culture plates and cultured for 24 h. Afterwards, cells were harvested and centrifuged, and supernatants were collected for the analysis of nitrite concentrations by a standard Griess assay. The cells were incubated without or with LPS (100 ng/mL) + nigericin (10 mM) together with the indicated concentrations of M8 or KG. Data are shown as the mean ± SEM and are representative of 2 independent experiments in triplicate for each well treatment condition ($n=6$). **B** M8 ($p>0.05$, $F=4.210$, df = 3), **C** KG ($p>0.05$, $F=6.120$, df = 3), **D** LPS + M8 ($p<0.001$, $F=8.980$, df = 3); **E** LPS + KG ($p<0.01$, $F=15.45$, df = 3), by one-way ANOVA followed by Tukey's post hoc test; $^{*}p<0.05$, $^{**}p<0.01$, $^{***}p<0.001$. ns, non-significant ($p>0.05$). $^{\#\#\#}p<0.001$ comparison between control and LPS + nigericin-treated group

cells was assessed by measuring the accumulated nitrite, a primary breakdown product of NO, using the Griess reaction assay. Cells were treated with LPS (100 ng/mL) + nigericin (10 mM) 30 min and incubated for 24 h, and the nitrite concentration in the medium increased significantly. Of note, after treating cells with M8 or KG at different concentrations, a significant concentration-dependent inhibition of NO secretion was observed (Fig. 2D and E).

Effect of M8 and KG on Cytokine Production and Phagocytosis

M8 and KG were also used to treat differentiated THP-1 cells to assess their inhibitory effect of pro-inflammatory cytokine IL-18 and IL-1β production. As shown in Fig. 3A and B (for M8) and in Fig. 3C and D (for KG), IL-18 and IL-1β levels in culture supernatants were significantly reduced by M8 and KG treatments compared to the LPS + nigericin group. As for the TAMRA-Aβ phagocytosis assay, both treatments significantly increased THP-1 cell phagocytic activities at 20 and 40 µM for M8, and at 100 µg/mL for KG, in comparison to the control not receiving the substance (Fig. 3E and F).

Effect of M8 and KG on Inflammasome Component Gene Expression

M8 was assessed for its potential effect of inflammasome component gene expressions and quantified using RTqPCR technique. Figure 4 shows that M8 significantly reduced gene expression at 10, 20, and 40 µM ($p<0.001$) for NFkB; at 20 and 40 µM for NLRP3 ($p<0.001$); and at 20 and 40 µM for Caspase-1 ($p<0.001$) and IL-1β. Inhibition

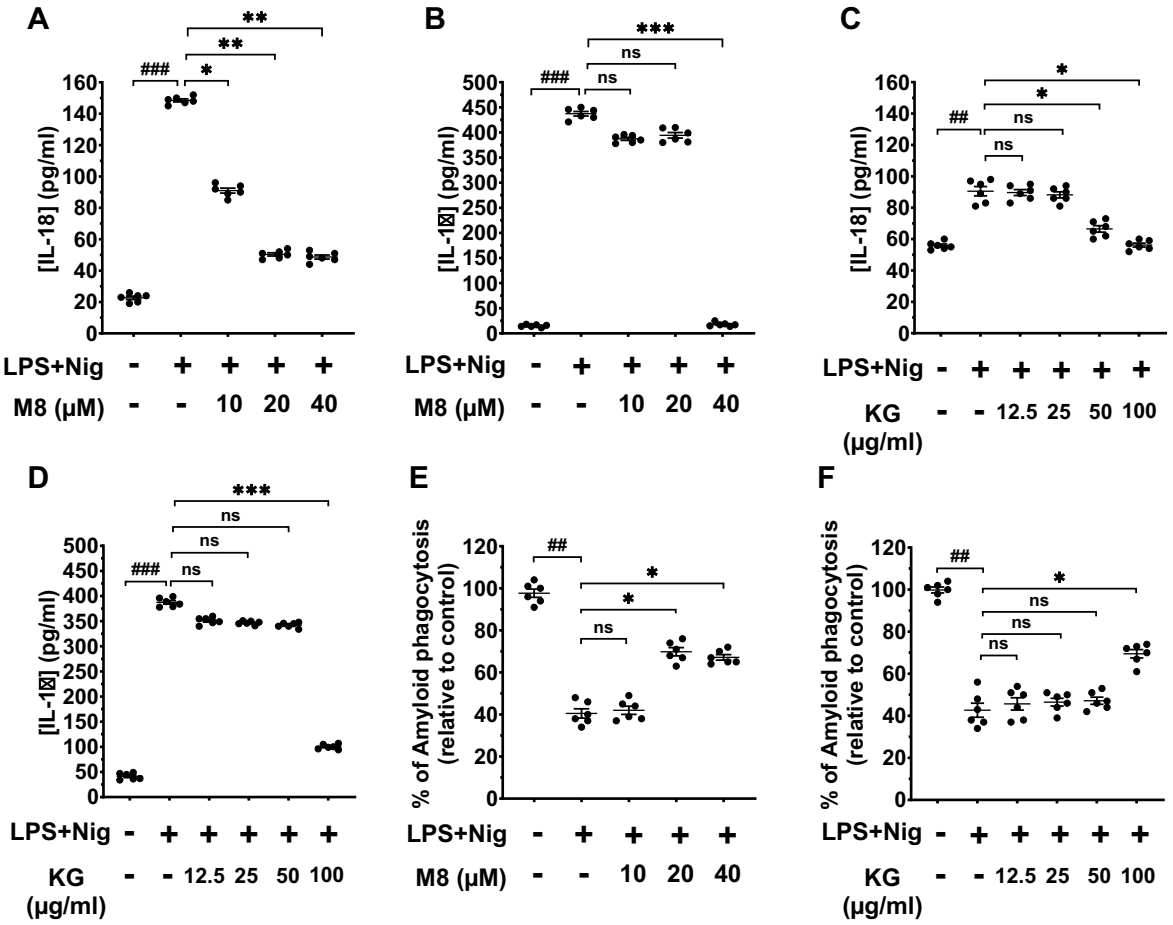

Fig. 3 ELISA and phagocytosis assays. **A**–**D** ELISA: effect of M8 or KG on the production of pro-inflammatory cytokines of LPS/nigericin-induced cells. THP-1 cells were grown in complete RPMI medium containing penicillin, streptomycin, and 10% FCS at 37 °C and 5% CO_2. 5×10^5 cells were seeded into 24-well cell culture plates and cultured for 24 h. THP-1 cells 5×10^5 cells/mL were incubated with the indicated concentrations of substances, in the presence or absence of LPS 100 ng/mL and nigericin 10 mM for 24 h. The cell supernatants were collected and used for ELISA. Each dot is the median of one-well cell culture supernatant from 2 independent experiments with 3 wells per treatment condition ($n=6$). **A** $p<0.01$, $F=17.0$, df = 3; **B** $p<0.001$, $F=12.34$, df = 3; **C** $p<0.05$, $F=11.45$, df = 3; **D** $p<0.001$, $F=9.678$, df = 3, by one-way ANOVA followed by Tukey's post hoc test. *$p<0.05$, **$p<0.01$, ***$p<0.001$. ns, non-significant ($p>0.05$). $^{\#}$Comparison between control and LPS-treated group. **E**, **F** Phagocytosis: effect of M8 or KG on TAMRA-Aβ phagocytosis. THP-1 cells were grown in complete RPMI medium containing penicillin, streptomycin, and 10% FCS at 37 °C and 5% CO_2. 5×10^5 cells were seeded into 96-well cell culture plates and cultured for 24 h. The cells were incubated without or with LPS 100 ng/mL and nigericin 10 mM, together with the indicated concentrations of M8 or KG. After 24 h, the phagocytosis was performed as described in the "Methods" section. Each dot is the median of one well from 2 independent experiments with 3 wells per treatment condition ($n=6$). **E** $p<0.001$, $F=8.159$, df = 3; **F** $p<0.05$, $F=17.0$, df = 3, by one-way ANOVA followed by Tukey's post hoc test. *$p<0.05$, **$p<0.01$, ***$p<0.001$. ns, non-significant ($p>0.05$). $^{\#\#}p<0.01$, $^{\#\#\#}p<0.001$ comparison between control and LPS + nigericin-treated group

of expression was only obtained at 40 µM for IL-18 compared to LPS + nigericin-treated cells. As far as KG effects on gene expression are concerned, expression was reduced at 25 µg/mL ($p<0.01$), 50 µg/mL ($p<0.001$), and 100 µg/mL ($p<0.001$) for NFkB and at 40 and 100 µg/mL for IL-1β and IL-18 respectively ($p<0.001$). Inhibition was observed at 25, 50 ($p<0.01$), and 100 ($p<0.001$) µg/mL for NLRP3 and at 25, 50, and 100 µg/mL for Caspase-1 ($p<0.001$), compared to LPS + nigericin-treated cells (Fig. 5).

Effect of M8 and KG on Inflammasome Component Protein Expression

We next investigated the effect of M8 and KG on the main inflammasome proteins (NFκBp65, NLRP3, pro-Caspase-1, and IL-1β) at their level of expression. Differentiated THP-1 cells were treated as described in the "Methods" section and protein levels were quantified by western blot. The results in Fig. 6 showed significant inhibition of most inflammasome components tested.

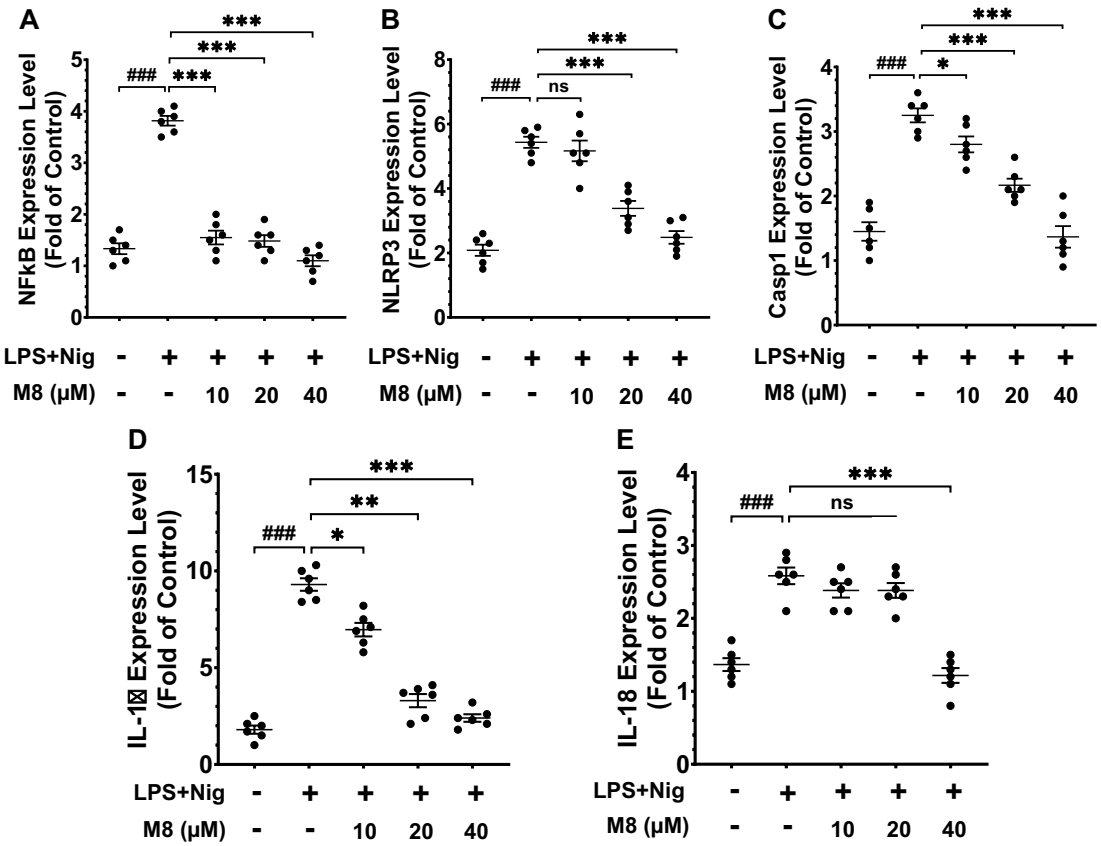

Fig. 4 M8 inhibits LPS-induced gene expression in THP-1 cells. THP-1 cells were treated with LPS (100 ng/mL) + nigericin (10 mM) followed by a treatment with M8 (10, 20, 40 μM). Thereafter, NFκB, NLRP3, Caspase-1, IL-1β, and IL-18 gene expression was assessed using RTqPCR. Each dot is the median of one well from 2 independent experiments with 3 wells per treatment condition. Data are expressed as mean ± SD ($n = 6$). **A** NFκB ($p < 0.01$, $F = 11.334$, df = 3), **B** NLRP3 ($p < 0.001$, $F = 10.517$, df = 3), **C** Caspase 1 ($p < 0.01$, $F = 17.761$, df = 3), **D** IL-1β ($p < 0.01$, $F = 13.567$, df = 3), **E** IL-18 ($p < 0.05$, $F = 6.712$, df = 3), by one-way ANOVA followed by Tukey's post hoc test. $^{*}p < 0.05$, $^{**}p < 0.01$, $^{***}p < 0.001$. ns, non-significant ($p > 0.05$). $^{\#\#\#}p < 0.001$ comparison between control and LPS + nigericin-treated group

Effect of M8 and KG on ASC Speck Formation

The ASC speck formation kinetically occurs after the inflammasome priming and formation, and is a relevant downstream inflammatory output to study. By taking advantage of the differentiated THP-1-ASC-GFP cells, which overexpress a human ASC protein fused with fluorescent GFP, it is possible to take images of the well under a fluorescent microscope to quantify the number and size of ASC specks still inside the microglia, or already released in the culture medium. As expected, LPS + nigericin treatment significantly increased the number of ASC specks compared to the control condition, and both M8 and KG pretreatments were able to significantly reduce this number back to the control level (Fig. 7A and B). Regarding the average size of the specks, no significant changes across the different conditions were observed (Fig. 7C). By analyzing the culture media via a flow cytometer, and by gating for the size of debris (Fig. 8A), we were able to compare the fluorescent intensity of the ASC specks between conditions (Fig. 8B). Overall, the median intensity of the ASC specks was the same in all the conditions, which is consistent with their unchanged size between conditions (Fig. 8C). Taken together, these results indicate that whatever the treatment, ASC specks are of the same size and fluorescent intensity, but that M8 and KG pretreatments were able to inhibit the increase of number of ASC speck formation due to LPS + Nig, inside and outside the macrophages.

Discussion

Flavonoids are phytochemicals naturally present in vegetables and fruits with well-known health benefits. In AD, flavonoids are reported to have neuroprotective effects by inhibiting the self-assembly of Aβ peptides into oligomers and have the capacity to slow the neuronal degeneration by being able to cross the blood–brain barrier [32]. Moreover,

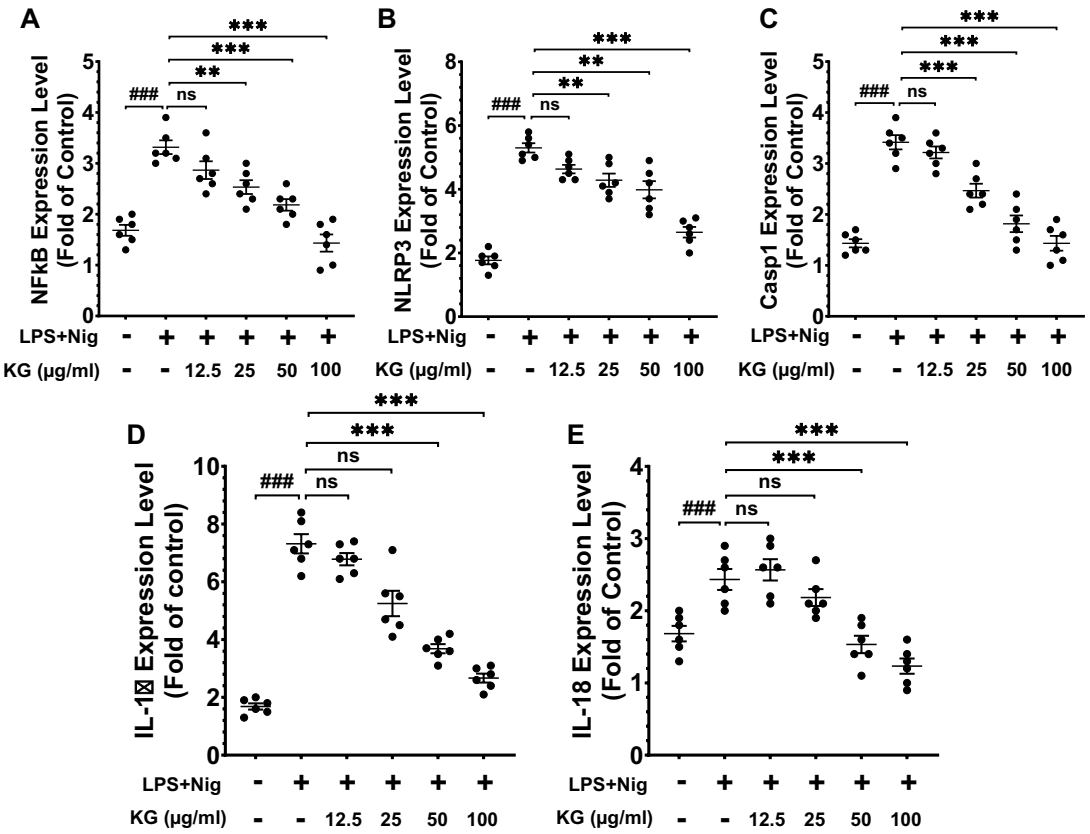

Fig. 5 KG inhibits LPS-induced gene expression in THP-1 cells. THP-1 cells were treated with LPS (100 ng/mL) + nigericin (10 mM) followed by a treatment with KG (12.5, 25, 50, and 100 µg/mL). Thereafter, NFκB, NLRP3, Caspase-1, IL-1β, and IL-18 gene expression was assessed using RTqPCR. Each dot is the median of one well from 2 independent experiments with 3 wells per treatment condition. Data are expressed as mean ± SD ($n=6$). **A** NFκB ($p<0.05$, $F=8.314$, df = 3), **B** NLRP3 ($p<0.01$, $F=10.517$, df = 3), **C** Caspase 1 ($p<0.001$, $F=18.145$, df = 3), **D** IL-1β ($p<0.001$, $F=9.159$, df = 3), **E** IL-18 ($p<0.05$, $F=12.210$, df = 3), by one-way ANOVA followed by Tukey's multiple comparison test. $^{*}p<0.05$, $^{**}p<0.01$, $^{***}p<0.001$. ns, non-significant ($p>0.05$). $^{\#\#\#}p<0.001$ comparison between control and LPS + nigericin-treated group

flavonoids are reported to slow neuronal degeneration, and therefore have a promising pharmacological effect in treating AD. Biflavonoids are a subclass of flavonoids formed by two identical or non-identical flavonoid units [33]. Nowadays, more attention has started to shift towards biflavonoids due to their advantages over monomeric flavonoids since they are able to survive first-pass metabolism which unfortunately inactivates most flavonoids [34]. Unlike flavonoids, biflavonoids' occurrence in nature is restricted to some species such as *Ochna* and *Campylospermum* [35]. Biflavonoids in recent studies have shown anticancer and antimicrobial activities [36, 37]. As far as AD is concerned, the few studies recently undertaken show that amentoflavone-like flavonoids have anti-amyloidogenic effects by inhibiting the aggregation of Aβ and promoting disaggregation of Aβ fibrils [38]. The NLRP3 inflammasome is the most studied member of the inflammasome protein family and a critical signaling step of the innate immune response. It mediates Caspase-1 activation, resulting in the secretion of pro-inflammatory interleukins 1β and 18. An aberrant activation of the NLRP3 inflammasome has been reported to have a crucial role in the development of AD and several other disorders including diabetes and atherosclerosis [39]. Unfortunately, no study has reported the effect of biflavonoids and KG on inflammasome regulation. The aim of this research work was to isolate biflavonoids from local medicinal plants as well as an extract of KG which has shown prominent anti-inflammatory activity in our previous work and study their capacity of inhibiting inflammasomes using well-known cell models of inflammation. In this study, the root bark of *Ochna schweinfurthiana* (Ochnaceae) was collected from Dang district in Adamaoua (Cameroon), and among the compounds isolated from the plant, the biflavonoid 7,7′-di-O-methylchamaejasmin was obtained. KG was harvested in the West region of Cameroon and identified at the country's national herbarium.

One of the first pieces of information to obtain while using lead compounds in vitro is to confirm there is no cytotoxicity. For this, differentiated THP-1 cells were treated

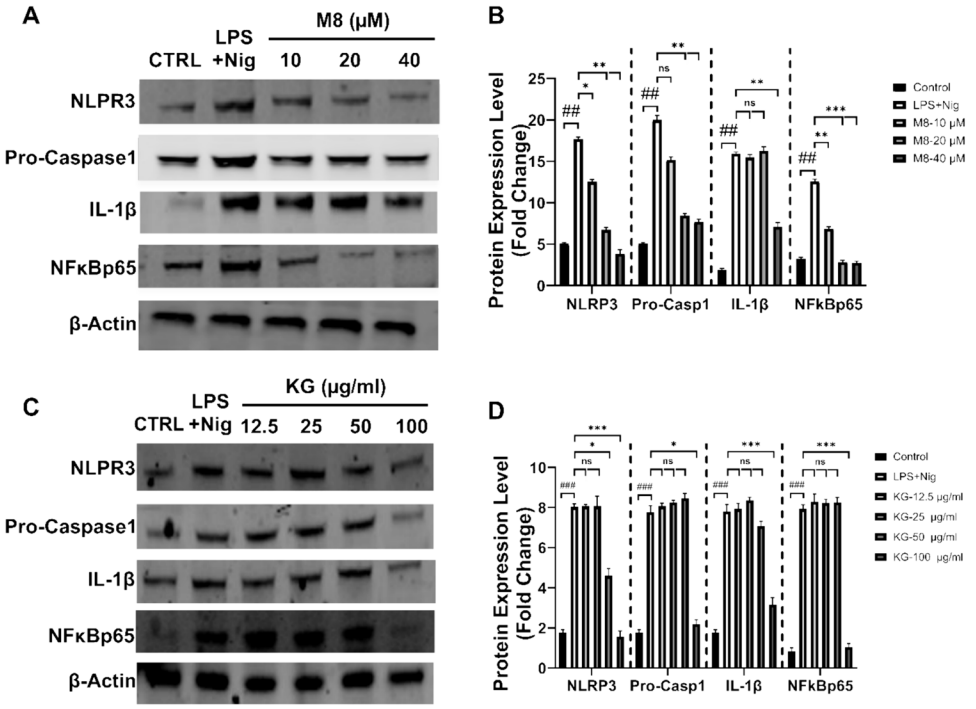

Fig. 6 Western blot analysis for NLRP3, pro-Caspase-1, IL-1β, and NFκBp65 protein level change with M8 and KG treatments. Compounds M8 and KG suppressed LPS + nigericin-induced NLRP3, pro-Caspase-1, IL-1β, and NFκBp65 inflammasome protein expression in THP-1 polarized macrophages. **A** + **C** Representative images of the western blots showing protein expression of NLRP3, pro-Caspase-1, IL-1β, and NFκBp65 with M8 or KG treatments. β-Actin was used as housekeeping protein. **B** Relative quantitation of NLRP3, pro-Caspase-1, IL-1β, and NFκBp65 levels with M8 treatments. Data are expressed as mean ± SD ($n = 3$). NLRP3 ($p < 0.01$, $F = 8.123$, df = 3), pro-Casp1 ($p < 0.05$, $F = 13.451$, df = 3), IL-1β ($p < 0.01$, $F = 11.13$, df = 3), NFκBp65 ($p < 0.001$, $F = 16.12$, df = 3), by one-way ANOVA followed by Tukey's multiple comparison test. $^{*}p < 0.05$, $^{**}p < 0.01$, $^{***}p < 0.001$. ns, non-significant ($p > 0.05$). **D** Relative quantitation of NLRP3, pro-Caspase-1, IL-1β, and NFκBp65 with KG treatments. Data are expressed as mean ± SD ($n = 3$). NLRP3 ($p < 0.001$, $F = 17.151$, df = 3), pro-Casp1 ($p < 0.01$, $F = 13.401$, df = 3), IL-1β ($p < 0.05$, $F = 8.33$, df = 3), NFκBp65 ($p > 0.05$, $F = 4.13$, df = 3), by one-way ANOVA followed by Tukey's multiple comparison test. $^{*}p < 0.05$, $^{**}p < 0.01$, $^{***}p < 0.001$. ns, non-significant ($p > 0.05$). $^{\#\#}p < 0.01$, $^{\#\#\#}p < 0.001$ comparison between control and LPS + nigericin-treated group

with increasing concentrations of M8 and as shown in Fig. 2A. Neither M8 nor KG did show any toxic effects on cells at the tested concentrations. In the following experiment, anti-inflammatory properties of substances were evaluated by studying their inhibitory effect after cell stimulation with bacterial lipopolysaccharide (LPS) and nigericin. Nigericin is a microbial toxin derived from the Gram-positive bacteria *Streptomyces hygroscopicus*. It is reported to be able to induce the release of IL-1β via NLRP3 inflammasome activation. On the other hand, THP-1 cell pretreatment with LPS initiates the activation of NLRP3 inflammasome in a phenomenon known as LPS priming. During the NLRP3 inflammasome action cascade, ASC specks (apoptosis-associated speck-like protein containing a CARD) are micrometer-sized structures formed as a hallmark of inflammasome activation. In immune cells (macrophages, monocytes), ASC adapter can be observed in the nucleus as they reach a size of around 1 μM. Many natural compounds including flavonoids have been reported to affect the inflammasome cascade even though the exact mechanism of action is still not clearly defined. This is the case of apigenin, quercetin, and kaempferol reported to inhibit ASC oligomerization without affecting the ASC level in cell lysates [40]. Similar results were reported with some plant crude extracts such as the ethanolic extract of *Artemisia anomala* with inhibited ASC oligomerization and ASC speck formation in immune cells [41]. However, no study has reported the effects of KG or M8 (biflavonoid) on inflammasome inhibition so far. Interestingly, and contrary to other reports, we revealed that these two substances can reduce the number of ASC specks formed (Fig. 7), the latter being often correlated with poor prognosis in diseases related to inflammasome activation such as AD.

In order to understand at which level the inflammasome activation was blocked by M8 and KG, RTqPCR and western blot were performed and revealed a reduction of inflammasome component gene expression as well as protein levels. An inhibition of Caspase-1 expression suggests a blockade at the level of caspase activation. A reduction of ASC speck formation and the inhibition of NFκB suggest that reduction

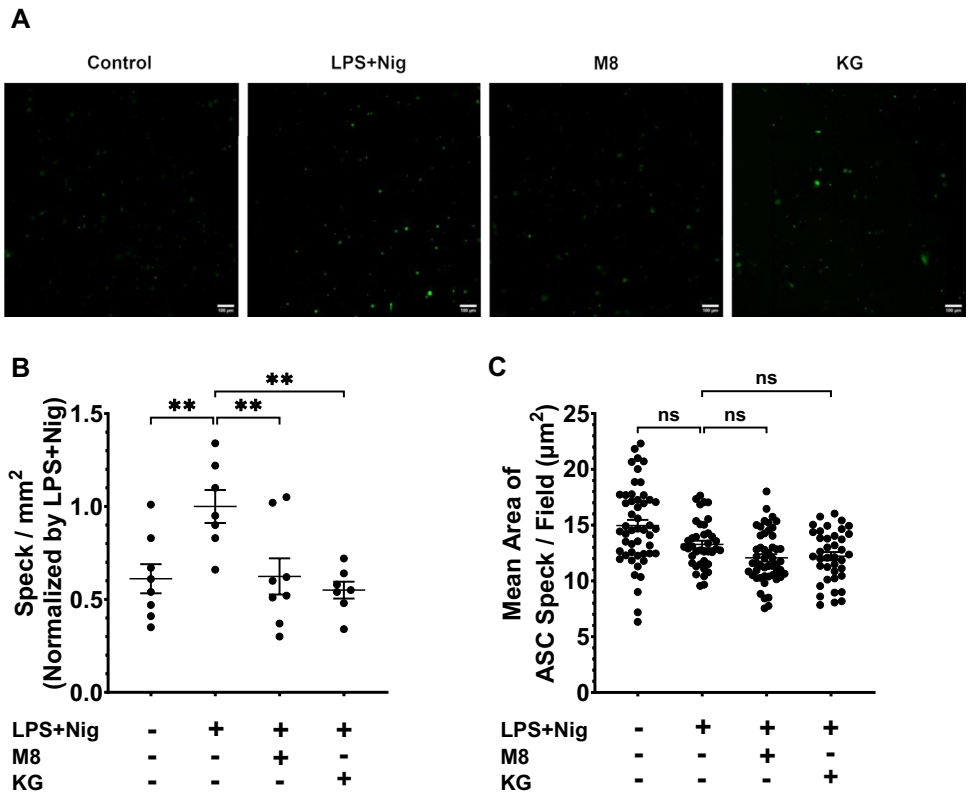

Fig. 7 KG and M8 inhibited ASC speck formation inside and outside differentiated THP-1-ASC-GFP cells. **A** After cell treatment as described in the "Methods" section, ASC specks were imaged under a Zeiss Axio Observer 7 microscope. The white scale bars represent 100 µm. **B** Quantification of the number of ASC-GFP specks per mm^2. Each dot is the mean value for one well, based on the values quantified for 1–10 images per well in 3 independent experiments with 2–3 wells per experiment. Data are expressed as mean ± SEM ($n = 7–8$). $^{**}p < 0.01$, by ordinary one-way ANOVA ($p = 0.0030$, $F = 5.990$, df = 3) followed by Dunnett's multiple comparisons test. **C** Quantification of the size of ASC-GFP specks per field of view. Each dot is the mean size of the specks on one image, for 39–50 images per condition in 3 independent experiments. Data are expressed as mean ± SEM ($n = 41–53$). ns, non-significant ($p > 0.05$), by one-way Kruskal–Wallis test ($p < 0.0001$, $\chi^2 = 25.73$, df = 3) followed by Dunnett's multiple comparisons test

in the expression of this transcription factor also contributes to inflammasome inhibition in this study. Other reports mention the inhibition of Nrf2 as contributing to inflammasome inhibition [42]. KG, which we demonstrated to have Nrf2 inhibitory properties in our previous work [28], may in addition to the results obtained in this study also inhibit inflammasome via Nrf2 and NFκB pathway blockade. Overall, the two plant-extracted substances investigated here appear to inhibit inflammasome activation at several levels. This includes inhibition of its main components at the gene and protein levels, and also via inhibition of upstream transcription factors.

The inflammatory response is known to play a critical role in AD, with reported upregulation of nitric oxide synthase responsible for nitric oxide production. In AD, Kummer et al. identified Aβ as an NO target, with nitration at tyrosine residue 10 (3NTyr(10)-Aβ) accelerating its aggregation [43], suggesting a crucial role of nitric oxide production for AD treatment and the potential beneficial role of our substances as lead drugs against AD.

The role of phagocytosis of Aβ plaques in AD has not been fully described; but several reports showed that Aβ impairs the phagocytic activity of brain microglia and astrocytes. Microglia are responsible for the removal of Aβ oligomers and fibrils by phagocytosis [44]. However, it was demonstrated that impairment of this process may lead to an increase in Aβ load which could later aggregate to form Aβ plaques [45]. Indeed, lysosomal accumulation of phagocytosed Aβ promotes its aggregation, resulting in lysosomal rupture and further release of IL-1β and IL-18 [46]. The capacity of our two substances to rescue phagocytic activity suggests they may protect the phagolysosome from Aβ injury and sustain macrophage phagocytic activity.

Overall, this study highlights for the first time the effects of a natural biflavonoid and a plant crude extract on NLRP3 inflammasome activation and will support our future studies aiming at analyzing their effects in vivo using transgenic mouse models of AD.

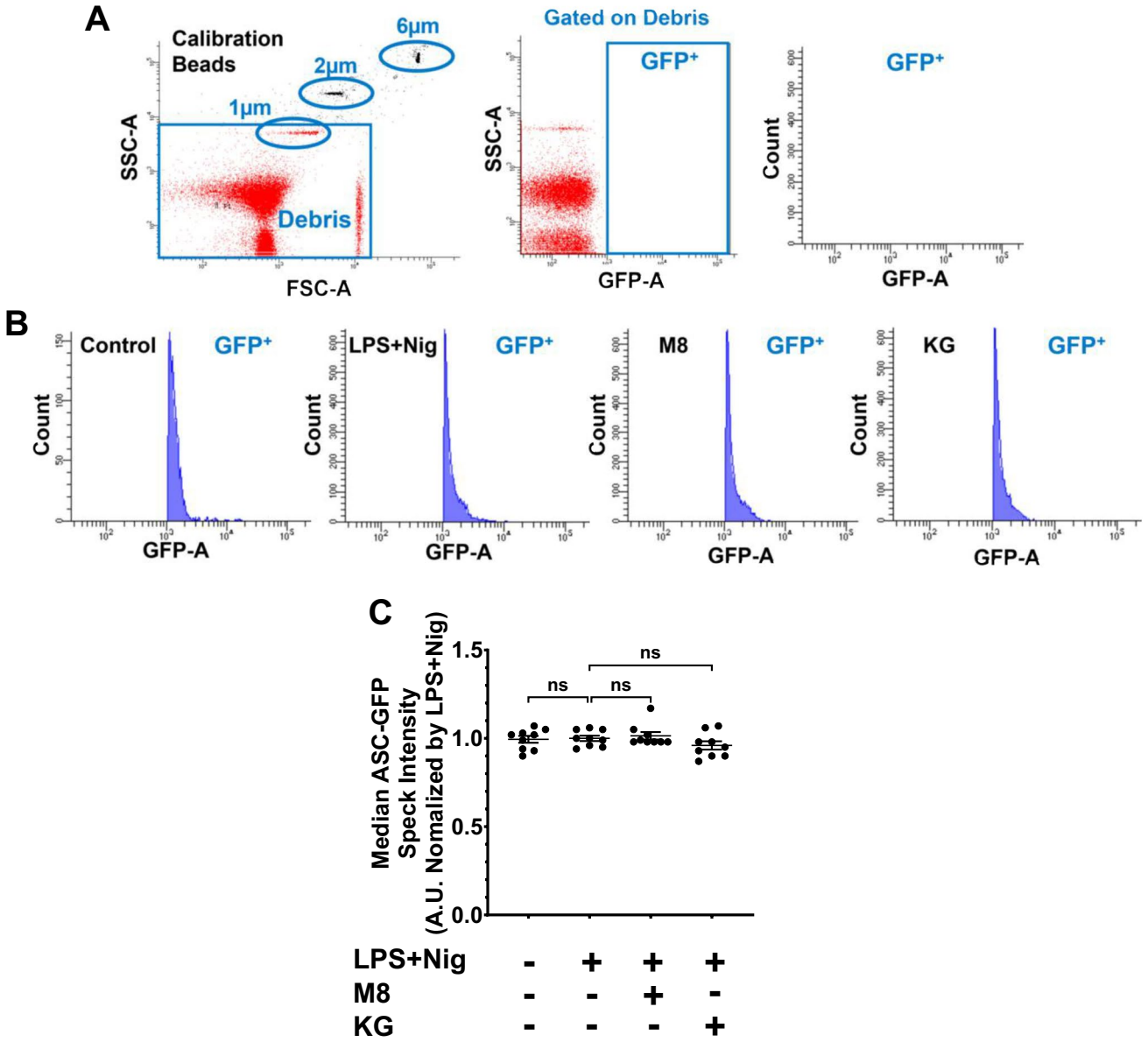

Fig. 8 KG and M8 effects on released ASC speck fluorescent intensity. **A** Flow cytometry gating strategy on 1-µm, 2-µm, and 6-µm non-fluorescent calibration beads. The first gating was done on the < 1-µm debris, and another one on the GFP^+ debris, which are not present in this condition. **B** Representative histograms of ASC-GFP^+ speck fluorescent intensity (arbitrary unit) across the different conditions. At least 2000 events were recorded. **C** Quantification of the median ASC-GFP^+ speck fluorescent intensity (arbitrary unit). Each dot is the median of one well's culture media from 3 independent experiments with 3 wells per experiment. Data are expressed as mean ± SEM ($n = 9$). ns, non-significant ($p > 0.05$), by one-way Kruskal–Wallis test ($p = 0.3783$, $\chi^2 = 3.088$, df = 3) followed by Dunn's multiple comparisons test

Author Contribution Brice Ayissi Owona designed the experiments, conducted the experiments, and wrote the manuscript. Arnaud Mary and Angelique N. Messi designed and conducted experiments and wrote the manuscript. Kishore Aravind Ravichandran conducted experiments. Josephine Ngo Mbing, Emmanuel Pegnyemb, Paul F. Moundipa, and Michael T. Heneka supervised the experiments and edited the manuscript.

Funding This study was financed by the TWAS-DFG Organization via the Postdoctoral fellowship #HE3350/19–1 awarded to Dr. Brice Ayissi Owona.

Data Availability The contact point for any data and/or material access requests are corresponding authors Brice Ayissi Owona (vincent-brice.

owona@facsciences-uy1.cm) and Michael T. Heneka (michael.heneka@uni.lu).

Declarations

Ethics Approval Not applicable.

Consent to Participate Not applicable.

Consent for Publication Not applicable.

Competing Interests The authors declare no competing interests.

References

1. Cacquevel M, Lebeurrier N, Chéenne S, Vivien D (2004) Cytokines in neuroinflammation and Alzheimer's disease. Curr Drug Targets 5:529–534. https://doi.org/10.2174/1389450043345308
2. Zetterberg H, Mattsson N, Shaw LM, Blennow K (2010) Biochemical markers in Alzheimer's disease clinical trials. Biomark Med 4:91–98. https://doi.org/10.2217/bmm.09.80
3. Schlachetzki J, Hull M (2009) Microglial activation in Alzheimer's disease. Curr Alzheimer Res 6:554–563. https://doi.org/10.2174/156720509790147179
4. Mandrekar-Colucci S, Landreth GE (2012) Microglia and inflammation in Alzheimer's disease. CNS Neurol Disord - Drug Targets 9:156–167. https://doi.org/10.2174/187152710791012071
5. Zhai X, Liu J, Ni A, Ye J (2020) MiR-497 promotes microglia activation and proinflammatory cytokines production in chronic unpredictable stress-induced depression via targeting FGF2. J Chem Neuroanat 110:101872–101894. https://doi.org/10.1016/j.jchemneu.2020.101872
6. Liu HD, Li W, Chen ZR et al (2013) Expression of the NLRP3 inflammasome in cerebral cortex after traumatic brain injury in a rat model. Neurochem Res 38:2072–2083. https://doi.org/10.1007/s11064-013-1115-z
7. Kalinin S, González-Prieto M, Scheiblich H et al (2018) Transcriptome analysis of alcohol-treated microglia reveals down-regulation of beta amyloid phagocytosis. J Neuroinflammation 15:141–156. https://doi.org/10.1186/s12974-018-1184-7
8. Lee JW, Nam H, Kim LE et al (2019) TLR4 (toll-like receptor 4) activation suppresses autophagy through inhibition of FOXO3 and impairs phagocytic capacity of microglia. Autophagy 15:753–770. https://doi.org/10.1080/15548627.2018.1556946
9. Heneka MT, Kummer MP, Stutz A et al (2013) NLRP3 is activated in Alzheimer's disease and contributes to pathology in APP/PS1 mice. Nature 493:674–678. https://doi.org/10.1038/nature11729
10. Huang Y, Jiang H, Chen Y et al (2018) Tranilast directly targets NLRP 3 to treat inflammasome-driven diseases. EMBO Mol Med 10:8689–8699. https://doi.org/10.15252/emmm.201708689
11. Toldo S, Mauro AG, Cutter Z et al (2019) The NLRP3 inflammasome inhibitor, OLT1177 (dapansutrile), reduces infarct size and preserves contractile function after ischemia reperfusion injury in the mouse. J Cardiovasc Pharmacol 73:215–222. https://doi.org/10.1097/FJC.0000000000000658
12. Yang H, Huang J, Gao Y et al (2020) Oridonin attenuates carrageenan-induced pleurisy via activation of the KEAP-1/Nrf2 pathway and inhibition of the TXNIP/NLRP3 and NF-κB pathway in mice. Inflammopharmacology 28:513–523. https://doi.org/10.1007/s10787-019-00644-y
13. Ward R, Li W, Abdul Y et al (2019) NLRP3 inflammasome inhibition with MCC950 improves diabetes-mediated cognitive impairment and vasoneuronal remodeling after ischemia. Pharmacol Res 142:237–250. https://doi.org/10.1016/j.phrs.2019.01.035
14. He X, Yang F, Huang X (2021) Proceedings of chemistry, pharmacology, pharmacokinetics and synthesis of biflavonoids. Molecules 26:6088–6101. https://doi.org/10.3390/molecules26196088
15. Andrade AWL, da Machado K, C, Machado K da C, et al (2018) In vitro antioxidant properties of the biflavonoid agathisflavone. Chem Cent J 12:75–91. https://doi.org/10.1186/s13065-018-0443-0
16. Terashima K, Shimamura T, Tanabayashi M, et al (1997) Constituents of the seeds of Garcinia kola: two new antioxidants, garcinoic acid and garcinal. Heterocycles 2–101–117. https://doi.org/10.3987/com-97-7854
17. de Freitas CS, Rocha MEN, Sacramento CQ et al (2019) Agathisflavone, a biflavonoid from Anacardium occidentale L., inhibits influenza virus neuraminidase. Curr Top Med Chem 20:111–120. https://doi.org/10.2174/1568026620666191219150738
18. Li F, Song X, Su G et al (2019) Amentoflavone inhibits HSV-1 and ACV-resistant strain infection by suppressing viral early infection. Viruses 15:466–487. https://doi.org/10.3390/v11050466
19. Park H, Kim YH, Chang HW, Kim HP (2010) Anti-inflammatory activity of the synthetic C-C biflavonoids. J Pharm Pharmacol 58:1661–1667. https://doi.org/10.1211/jpp.58.12.0014
20. Thapa A, Woo ER, Chi EY et al (2011) Biflavonoids are superior to monoflavonoids in inhibiting amyloid-β toxicity and fibrillogenesis via accumulation of nontoxic oligomer-like structures. Biochemistry 50:2445–2455. https://doi.org/10.1021/bi101731d
21. Sirimangkalakitti N, Juliawaty LD, Hakim EH et al (2019) Naturally occurring biflavonoids with amyloid β aggregation inhibitory activity for development of anti-Alzheimer agents. Bioorg Med Chem Lett 29:1994–1997. https://doi.org/10.1016/j.bmcl.2019.05.020
22. Choi EY, Kang SS, Lee SK, Han BH (2020) Polyphenolic biflavonoids inhibit amyloid-beta fibrillation and disaggregate preformed amyloid-beta fibrils. Biomol Ther 28:145–151. https://doi.org/10.4062/biomolther.2019.113
23. Thapa A, Chi EY (2015) Biflavonoids as potential small molecule therapeutics for Alzheimer's disease. Adv Exp Med Biol 863–55–77. https://doi.org/10.1007/978-3-319-18365-7_3
24. Adem FA, Mbaveng AT, Kuete V et al (2019) Cytotoxicity of isoflavones and biflavonoids from Ormocarpum kirkii towards multifactorial drug resistant cancer. Phytomedicine 58:152853–152864. https://doi.org/10.1016/j.phymed.2019.15285
25. Chukwujekwu JC, De Kock CA, Smith PJ et al (2012) Antiplasmodial and antibacterial activity of compounds isolated from Ormocarpum trichocarpum. Planta Med 78:1857–1860. https://doi.org/10.1055/s-0032-1315386
26. Galani BRT, Sahuc M-E, Sass G et al (2016) Khaya grandifoliola C.DC: a potential source of active ingredients against hepatitis C virus in vitro. Arch Virol 161:1169–1181. https://doi.org/10.1007/s00705-016-2771-5
27. Kouam AF, Njayou FN, Yuan F et al (2021) Inhibitory activity of limonoids from Khaya grandifoliola C.DC (Meliaceae) against hepatitis C virus infection in vitro. Avicenna J Phytomedicine 11:353–366. https://doi.org/10.22038/AJP.2020.17215
28. Njayou FN, Amougou AM, Fouemene Tsayem R et al (2015) Antioxidant fractions of Khaya grandifoliola C.DC. and Entada africana Guill. et Perr. induce nuclear translocation of Nrf2 in HC-04 cells. Cell Stress Chaperones 20:991–1000. https://doi.org/10.1007/s12192-015-0628-6
29. Owona BA, Njayou FN, Mkounga P, Moundipa PF (2022) Khaya grandifoliola active fraction as a source of therapeutic compounds for Alzheimer's disease treatment: in silico validation of identified

compounds. Silico Pharmacol 10:11. https://doi.org/10.1007/s40203-022-00126-0
30. Tsikas D (2007) Analysis of nitrite and nitrate in biological fluids by assays based on the Griess reaction: appraisal of the Griess reaction in the l-arginine/nitric oxide area of research. J Chromatogr B 851:51–70. https://doi.org/10.1016/j.jchromb.2006.07.054
31. Stutz A, Horvath GL, Monks BG, Latz E (2013) ASC speck formation as a readout for inflammasome activation. In: De Nardo CM, Latz E (eds) The inflammasome. Humana Press, Totowa, NJ, pp 91–101
32. Kaur R, Sood A, Lang DK et al (2022) Potential of flavonoids as anti-Alzheimer's agents: bench to bedside. Environ Sci Pollut Res Int 29:26063–26077. https://doi.org/10.1007/s11356-021-18165-z
33. Patel K, Singh GK, Patel DK (2018) A review on pharmacological and analytical aspects of naringenin. Chin J Integr Med 24:551–560. https://doi.org/10.1007/s11655-014-1960-x
34. Komoto N, Nakane T, Matsumoto S et al (2015) Acyl flavonoids, biflavones, and flavonoids from Cephalotaxus harringtonia var. nana. J Nat Med 69:479–486. https://doi.org/10.1007/s11418-015-0912-x
35. Djova SV, Nyegue MA, Messi AN et al (2019) Phytochemical study of aqueous extract of Ochna schweinfurthiana F. Hoffm powder bark and evaluation of their anti-inflammatory, cytotoxic, and genotoxic properties. Evid-Based Complement Altern Med ECAM 2019:8908343. https://doi.org/10.1155/2019/8908343
36. Menezes JCJMDS, Campos VR (2021) Natural biflavonoids as potential therapeutic agents against microbial diseases. Sci Total Environ 769:145168. https://doi.org/10.1016/j.scitotenv.2021.145168
37. Li M, Li B, Xia Z-M et al (2019) Anticancer effects of five biflavonoids from Ginkgo biloba L. male flowers in vitro. Mol Basel Switz 24:1496. https://doi.org/10.3390/molecules24081496
38. Windsor PK, Plassmeyer SP, Mattock DS et al (2021) Biflavonoid-induced disruption of hydrogen bonds leads to amyloid-β disaggregation. Int J Mol Sci 22:2888. https://doi.org/10.3390/ijms22062888
39. Huang Y, Xu W, Zhou R (2021) NLRP3 inflammasome activation and cell death. Cell Mol Immunol 18:2114–2127. https://doi.org/10.1038/s41423-021-00740-6
40 Lim Hyun, Dong SM, Haeil P, Hyun PK (2018) Flavonoids interfere with NLRP3 inflammasome activation. Toxicol Appl Pharmacol 355:93–102. https://doi.org/10.1016/j.taap.2018.06.022
41. Feng H, Min Z, Lil X, et al (2022) The ethanolic extract of Artemisia anomala exerts anti-inflammatory effects via inhibition of NLRP3 inflammasome. Phytomedicine Int J Phytother Phytopharm 102:. https://doi.org/10.1016/j.phymed.2022.154163-15417
42. Yan Z, Qi W, Zhan J et al (2020) Activating Nrf2 signalling alleviates osteoarthritis development by inhibiting inflammasome activation. J Cell Mol Med 24:13046–13057. https://doi.org/10.1111/jcmm.15905
43. Kummer MP, Hermes M, Delekarte A et al (2011) Nitration of tyrosine 10 critically enhances amyloid β aggregation and plaque formation. Neuron 71:833–844. https://doi.org/10.1016/j.neuron.2011.07.001
44. Hofbauer D, Mougiakakos D, Broggini L et al (2021) β2-Microglobulin triggers NLRP3 inflammasome activation in tumor-associated macrophages to promote multiple myeloma progression. Immunity 54:1772-1787.e9. https://doi.org/10.1016/j.immuni.2021.07.002
45. Hickman SE, Allison EK, El Khoury J (2008) Microglial dysfunction and defective beta-amyloid clearance pathways in aging Alzheimer's disease mice. J Neurosci Off J Soc Neurosci 28:8354–8360. https://doi.org/10.1523/JNEUROSCI.0616-08.2008
46. Sita G, Graziosi A, Hrelia P, Morroni F (2021) NLRP3 and infections: β-amyloid in inflammasome beyond neurodegeneration. Int J Mol Sci 22:6984. https://doi.org/10.3390/ijms22136984